

Supporting Information for ”The Tractrix Magnetopause: A Novel Physics-Based Functional Form for the Magnetopause Shape”

C. J. O’Brien¹, M. R. Collier², B.M. Walsh¹, D.G. Sibeck², E. Taylor³

¹Center for Space Physics, Boston University, Boston, MA, USA

²NASA/GSFC, Greenbelt, MD, USA

³Howard University, Washington, DC, USA

Contents of this file

1. Figures S1 to S4

Introduction

Below are supporting figures giving additional insight into the structure of the tractrix model and how that structure compares to the other models in this study, as well as figures showing the mean and standard deviation of the dynamic pressure in the magnetopause crossing dataset.

References

- Chao, J., Wu, D., Lin, C.-H., Yang, Y.-H., Wang, X., Kessel, M., ... Lepping, R. (2002). Models for the size and shape of the earth’s magnetopause and bow shock. In *COSPAR Colloquia Series* (Vol. 12, pp. 127–135). Elsevier. Retrieved 2020-05-
-

11, from <https://linkinghub.elsevier.com/retrieve/pii/S0964274902802128>
doi: 10.1016/S0964-2749(02)80212-8

Lin, R. L., Zhang, X. X., Liu, S. Q., Wang, Y. L., & Gong, J. C. (2010, April). A three-dimensional asymmetric magnetopause model: THREE-DIMENSIONAL MAGNETOPAUSE MODEL. *Journal of Geophysical Research: Space Physics*, *115*(A4), n/a–n/a. Retrieved 2020-03-12, from <http://doi.wiley.com/10.1029/2009JA014235>
doi: 10.1029/2009JA014235

Petrinec, S. M., & Russell, C. T. (1996, January). Near-Earth magnetotail shape and size as determined from the magnetopause flaring angle. *Journal of Geophysical Research: Space Physics*, *101*(A1), 137–152. Retrieved 2020-05-11, from <http://doi.wiley.com/10.1029/95JA02834> doi: 10.1029/95JA02834

Shue, J.-H., Song, P., Russell, C. T., Steinberg, J. T., Chao, J. K., Zastenker, G., ... Kawano, H. (1998, August). Magnetopause location under extreme solar wind conditions. *Journal of Geophysical Research: Space Physics*, *103*(A8), 17691–17700. Retrieved 2020-05-11, from <http://doi.wiley.com/10.1029/98JA01103>
doi: 10.1029/98JA01103

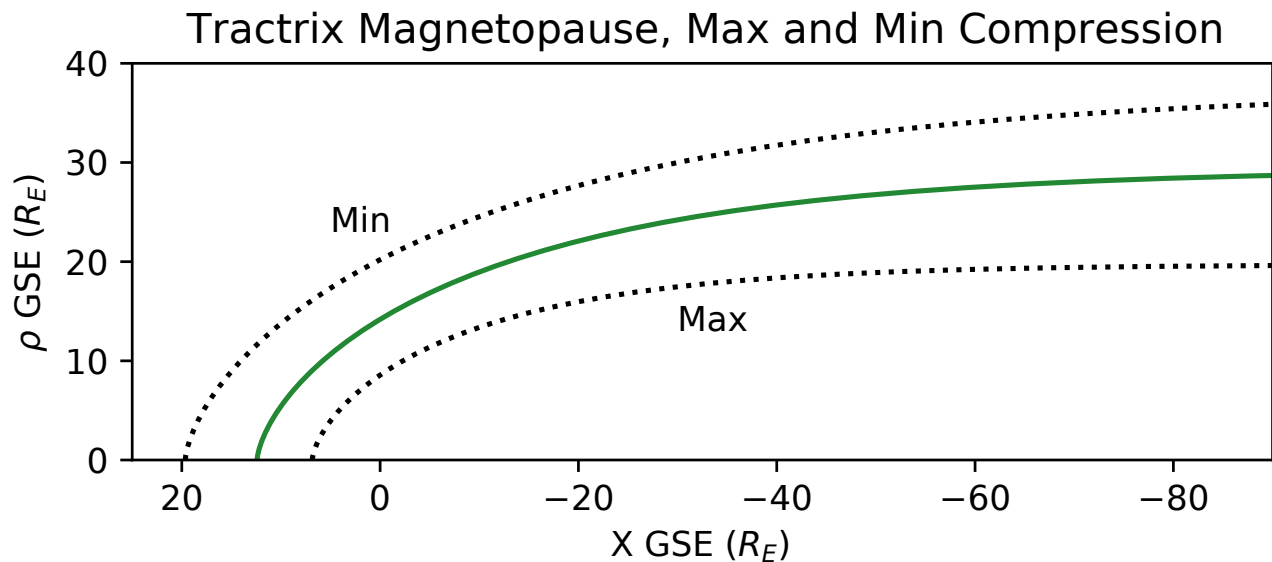


Figure S1. The tractrix model surface for mean values of B_S and P_{dyn} ($2.64nT$ and $2.40nPa$), as well as for maximum and minimum compression. Maximum compression corresponds to the maximum values of B_S and P_{dyn} ($17.0nT$ and $58.2nPa$). Minimum compression corresponds to the minimum values of B_S and P_{dyn} ($0.00nT$ and $0.182nPa$).

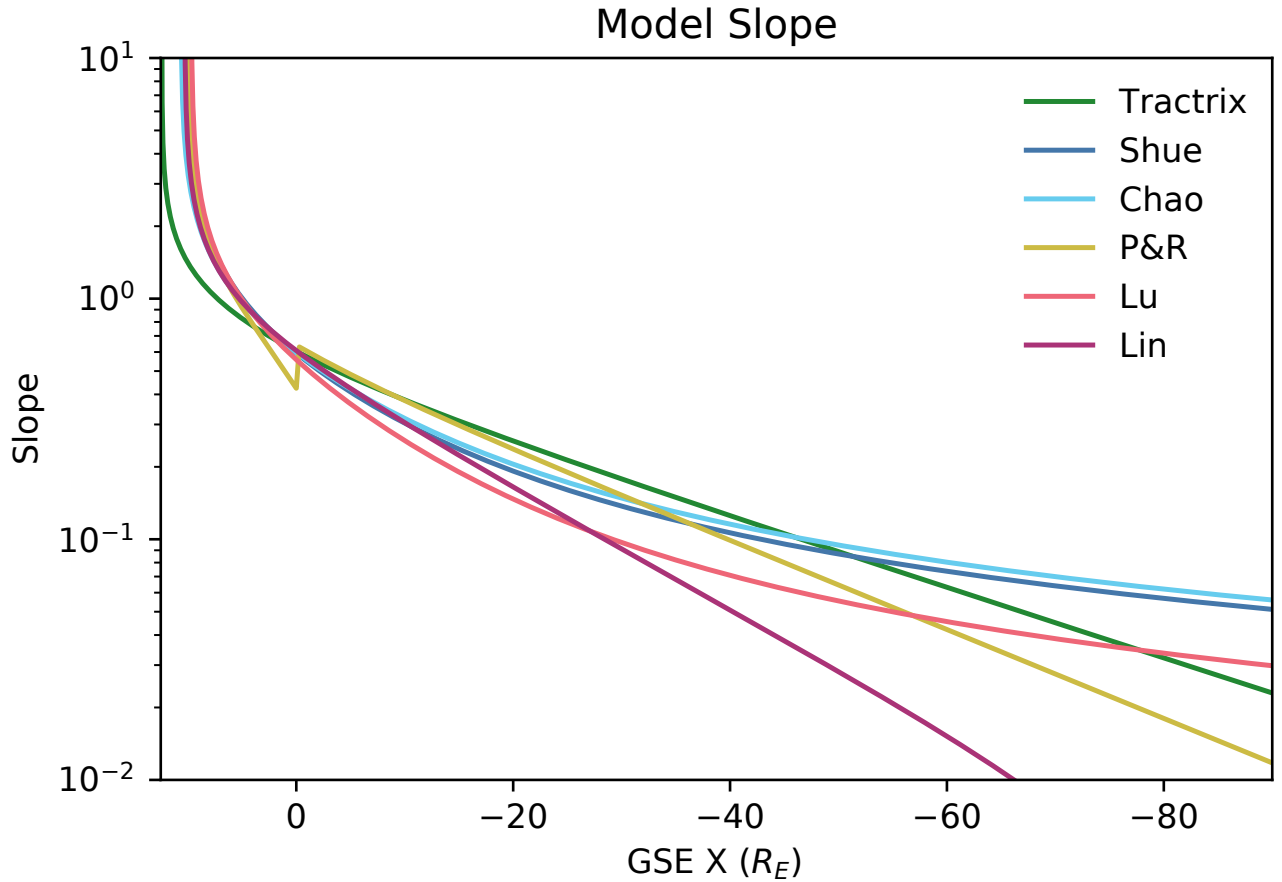


Figure S2. Slope of model curves for each model considered in this study. On the nightside, the tractrix has a larger slope than any other model until about $-45R_E$ GSE X, after which models that flare outward strongly (Shue et al. (1998), Chao et al. (2002)) overtake the tractrix's downtail expansion rate. Lin et al. (2010) and Petrinec and Russell (1996) always expand more slowly than the tractrix over reasonable distances downtail. Note the small discontinuity at $-45R_E$ GSE X for Petrinec and Russell (1996) where the model switches from its dayside functional form to its nightside functional form.

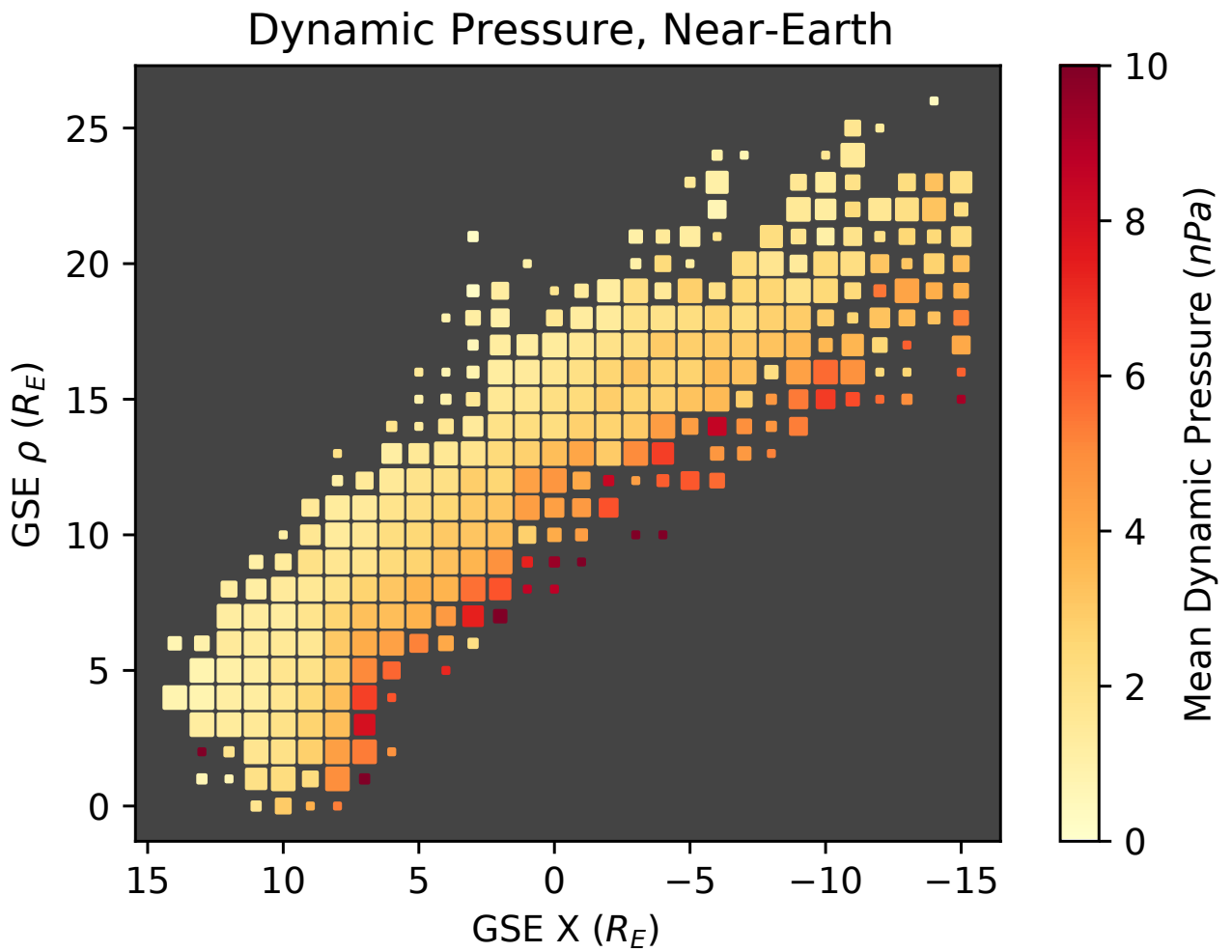


Figure S3. Mean solar wind dynamic pressure associated with each crossing, binned using the same scheme as Figure 10 in the main text. Note that the closest crossings to the Earth in the nose happen for extreme solar wind dynamic pressure, likely contributing to Chao et al. (2002) outperforming the tractrix in this region due to its specialized training dataset.

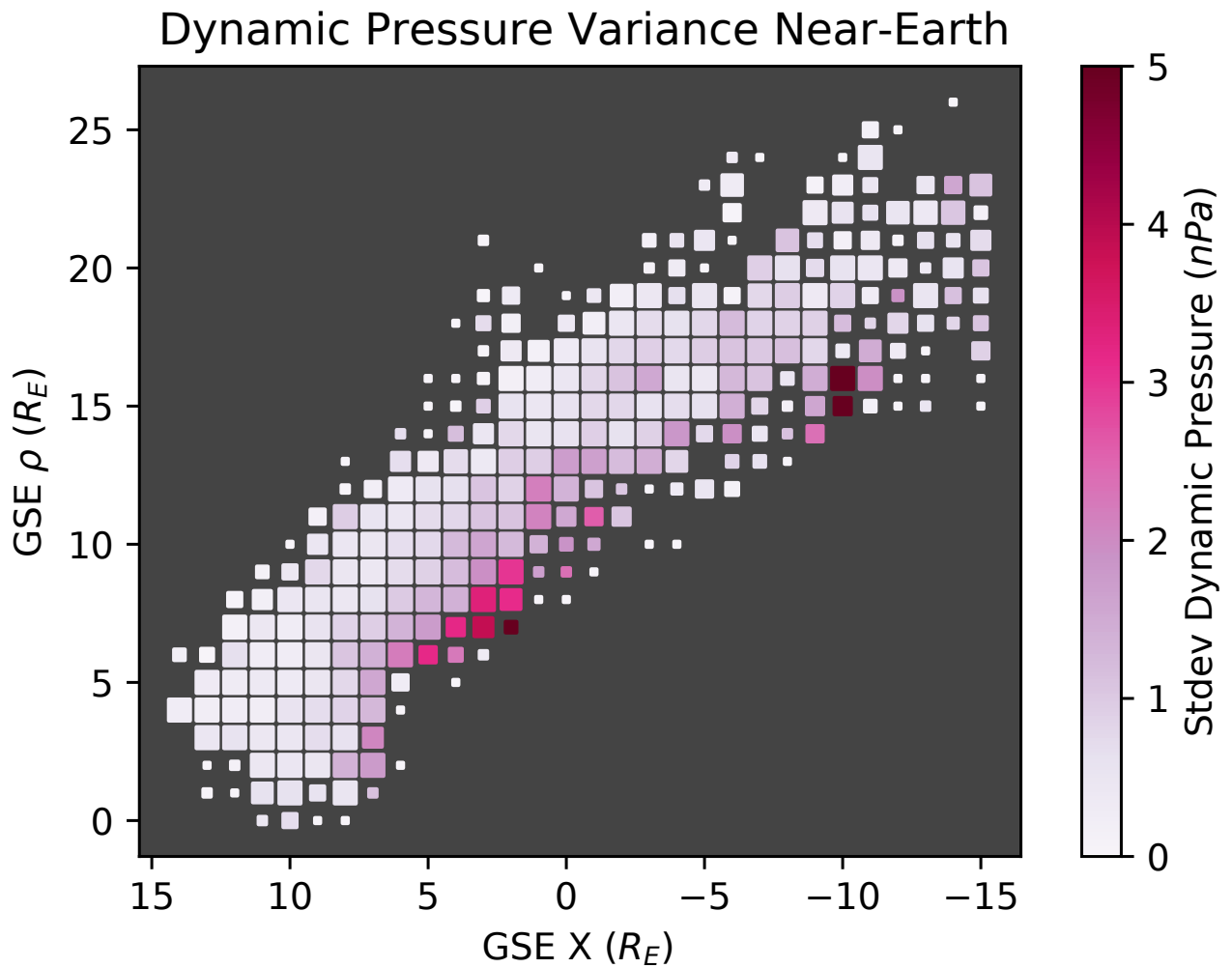


Figure S4. Standard deviation of solar wind dynamic pressure associated with each crossing, binned using the same scheme as Figure 10 in the main text.